

# Cross-modal Fuzzy Alignment Network for Text-Aerial Person Retrieval and A Large-scale Benchmark

Yifei Deng<sup>1,2</sup>, Chenglong Li<sup>1,\*</sup>, Yuyang Zhang<sup>4</sup>, Guyue Hu<sup>3</sup>, Jin Tang<sup>2</sup>

<sup>1</sup>State Key Laboratory of Opto-Electronic Information Acquisition and Protection Technology

<sup>2</sup>School of Computer Science and Technology, Anhui University

<sup>3</sup>School of Artificial Intelligence, Anhui University <sup>4</sup>The University of Hong Kong

{yf-ah, lc11314}@foxmail.com u3604018@connect.hku.hk {guyue.hu, tangjin}@ahu.edu.cn

## Abstract

Text-aerial person retrieval aims to identify targets in UAV-captured images from eyewitness descriptions, supporting intelligent transportation and public security applications. Compared to ground-view text-image person retrieval, UAV-captured images often suffer from degraded visual information due to drastic variations in viewing angles and flight altitudes, making semantic alignment with textual descriptions very challenging. To address this issue, we propose a novel Cross-modal Fuzzy Alignment Network, which quantifies the token-level reliability by fuzzy logic to achieve accurate fine-grained alignment and incorporates ground-view images as a bridge agent to further mitigate the gap between aerial images and text descriptions, for text-aerial person retrieval. In particular, we design the Fuzzy Token Alignment module that employs the fuzzy membership function to dynamically model token-level association strength and suppress the influence of unobservable or noisy tokens. It can alleviate the semantic inconsistencies caused by missing visual cues and significantly enhance the robustness of token-level semantic alignment. Moreover, to further mitigate the gap between aerial images and text descriptions, we design a Context-Aware Dynamic Alignment module to incorporate the ground-view agent as a bridge in text-aerial alignment and adaptively combine direct alignment and agent-assisted alignment to improve the robustness. In addition, we construct a large-scale benchmark dataset called AERI-PEDES by using a chain-of-thought to decompose text generation into attribute parsing, initial captioning, and refinement, thus boosting textual accuracy and semantic consistency. Experiments on AERI-PEDES and TBAPR demonstrate the superiority of our method. The dataset and code are available at: <https://github.com/Yifei-AHU/AERI-PEDES>



Figure 1. (a) Illustration of the text-aerial person retrieval task. (b) Semantically identical targets with substantial viewpoint discrepancies between ground and aerial perspectives. (c) Incomplete visual cues in aerial images result in only partial alignment with the corresponding captions.

## 1. Introduction

With the rapid advancement of deep learning [46] [21] [22] [31] [8] [24] and vision-language models [35] [18] [41] [2] [26], Text-Image Person Retrieval (TIPR) has attracted increasing attention in recent years. TIPR aims to accurately retrieve target individuals from image databases based on captions, with important applications in intelligent surveillance and traffic management [10] [15] [16]. However, all existing TIPR

\*Corresponding author.

studies [17] [4] [23] [32] rely on data captured by fixed ground-based cameras, which limits the coverage of person observation and makes it difficult to capture dynamic scenes in complex environments. The widespread adoption of unmanned aerial vehicles (UAVs) offers unique advantages for person monitoring. UAVs can capture scenes dynamically from multiple angles and locations, covering areas inaccessible to ground cameras and providing richer information sources. Building on the flexibility and wide-area coverage of UAVs, extending the TIPR task to aerial image scenarios captured by UAVs holds significant research value and practical importance. This direction not only helps address the challenges of cross-modal matching and semantic alignment in complex environments but also fully unleashes the potential of UAVs in applications such as intelligent traffic management, public safety, and security surveillance. To advance this line of research, Wang et al. [38] are the first to explore the problem of person retrieval from aerial perspectives and proposed the Text-Aerial Person Retrieval (TAPR) task, as shown in Figure 1(a).

Different from conventional TIPR, which only needs to address cross-modal semantic alignment between text and images, person images captured from aerial views exhibit nonlinear distortions in appearance, body posture, and geometric proportions due to extreme variations in shooting angle and altitude, as illustrated in Figure. 1(b). This significantly increases the difficulty of aligning them with textual descriptions. Moreover, query texts are typically derived from eyewitness descriptions and contain more complete and fine-grained person attributes and appearance details. However, in drone-captured scenarios, visual cues of persons are often sparse or even partially missing due to factors such as altitude, viewpoint deviation, and occlusion. As shown in Figure. 1(c), persons in aerial views only cover part of the semantic regions described in the text (highlighted in orange), whereas persons in ground views can fully correspond to the textual description. This inconsistency in visibility can lead to missing effective visual correspondences for some text tokens when constructing token-level fine-grained associations, thereby introducing erroneous cross-modal alignments.

To address the aforementioned challenges, we propose a Cross-Modal Fuzzy Alignment Network (CFAN), which leverages fuzzy logic to quantify token-level reliability for fine-grained alignment and incorporates ground-view images as a bridging proxy to further reduce the gap between aerial images and captions. Specifically, to mitigate the impact of visual discrepancies caused by aerial images captured at different altitudes on cross-modal alignment, we design a Context-Aware Dynamic Alignment (CDA) module. By using ground images as a bridge, this module quantifies the alignment difficulty between text-aerial and

text-ground images, and dynamically adjusts the contributions of direct alignment and bridged alignment, thereby enhancing the stability of text-aerial image alignment. Moreover, to address semantic inconsistencies in fine-grained alignment caused by missing visual cues, we propose a Fuzzy Token Alignment (FTA) module. This module dynamically models token-level association strength via fuzzy membership functions while suppressing unobservable or noisy tokens, significantly improving the robustness of token-level semantic alignment.

To further advance research on TAPR task, we construct a large-scale benchmark, AERI-PEDES, which contains 112,672 person images captured from diverse cameras and varied scenarios. For caption, to reduce manual annotation costs, we design a Chain-of-Thought (CoT) [40] based generation framework that decomposes the caption generation task into structured reasoning steps using multimodal language models, ensuring the generated training captions are rich in fine-grained attributes and visually consistent. To better reflect real-world applications, the test captions are manually annotated to ensure natural semantic expression, allowing the evaluation results to accurately reflect the true performance of the models. Extensive experiments on two text-aerial person retrieval benchmarks have thoroughly validated the effectiveness of the proposed method. In summary, the main contributions of this paper are as follows:

- We propose a Cross-modal Fuzzy Alignment Network, which quantifies the token-level reliability by fuzzy logic to achieve accurate fine-grained alignment, and incorporates ground-view images as a bridge agent to further mitigate the gap of text-aerial image.
- We design a Context-Aware Dynamic Alignment module, which incorporates ground images as a bridge and quantifies alignment difficulty to adaptively balance direct and bridged alignment, achieving robust cross-modal alignment.
- We introduce the Fuzzy Token Alignment module, which models token-level reliability with a fuzzy membership function, enhancing shared token alignment while suppressing non-shared alignment, leading to improved fine-grained alignment.
- We construct a large-scale benchmark, AERI-PEDES, and develop a Chain-of-Thought based caption generation framework to produce fine-grained, visually consistent captions.

## 2. Related Work

### 2.1. Text-Image Person Retrieval

TIPR aims to accurately locate corresponding person images from a gallery based on natural language descriptions. The task is first introduced by Li et al. [23], who establish the CUHK-PEDES dataset, laying the foundation for

cross-modal person retrieval research. Subsequently, extended benchmarks such as ICFG-PEDES [48] and RST-PRaid [7] are released, further advancing TIPR toward more realistic scenarios. Early studies mainly rely on global feature alignment [47], which reduces the modality gap between vision and language by constructing a joint embedding space. However, these approaches typically focus on salient regions, making it difficult to capture fine-grained cross-modal semantic correspondences. To address this, later works gradually shift toward local feature matching. For instance, Chen et al. [3] capture richer semantic information through multi-scale features to achieve adaptive cross-modal alignment, while Wang et al. [39] explore the association between human attributes and text, effectively improving fine-grained alignment accuracy. In recent years, the development of Vision-Language Pre-trained Models [33] [20] [19] has further driven TIPR research. Methods based on large-scale pre-trained models such as CLIP explore multi-layer semantic mining [43], image-guided language reconstruction [13], and hierarchical supervision from unimodal teachers [5], significantly enhancing cross-modal alignment accuracy and generalization. Moreover, pre-training with large-scale image-text data generated by diffusion models or VLMs [36] [44] [14] also substantially improves retrieval robustness.

## 2.2. Fuzzy Deep Learning

Fuzzy logic, originally proposed by Lotfi Zadeh [45], aims to characterize the inherent uncertainty and ambiguity of the real world. In recent years, researchers have integrated fuzzy logic with neural networks, forming the paradigm of Fuzzy Deep Learning. This integration endows models with the ability to reason under uncertainty and ambiguity, demonstrating remarkable advantages in fields such as medical image analysis [12] [11] and cross-modal retrieval [9]. Compared with traditional deep learning, fuzzy deep learning excels at modeling fuzzy boundaries and quantifying model uncertainty. For example, Ding et al. [6] introduced fuzzy adjacency information to optimize MRI brain structure segmentation. Akram et al. [1] proposed bipolar fuzzy neurons to achieve more accurate medical diagnoses; Nan et al. [27] incorporated fuzzy logic into attention mechanisms to construct a fuzzy attention network for airway segmentation, significantly improving segmentation performance. In the field of cross-modal retrieval, Duan et al. [9] proposed the Fuzzy Multimodal Learning framework based on fuzzy set theory, achieving more reliable retrieval through self-estimated cognitive uncertainty. Xu et al. [42] introduced a hypergraph-based residual fuzzy alignment network for open-set 3D cross-modal retrieval, significantly improving generalization.

## 3. Method

### 3.1. Overview

Figure 2 illustrates our proposed Cross-Modal Fuzzy Alignment Network, which consists of two modules, the Context-Aware Dynamic Alignment (CDA) module and the Fuzzy Token Alignment (FTA) module. We employ a shared CLIP image encoder to extract aerial person image features  $A$  and ground-level person image features  $G$ , and a CLIP text encoder to extract person description features  $T$ . The CDA module takes the global representations of aerial features  $A^c$ , ground features  $G^c$ , and text features  $T^c$  as input. It evaluates the alignment difficulty of each sample by comparing text-aerial and text-ground similarities, and dynamically modulates the contributions of direct and bridge-mediated alignment, thereby achieving robust sample-level cross-modal alignment. The FTA module takes  $A$  and  $T$  as input and introduces a fuzzy membership function at the token level to assign each token a continuous existence degree. Multi-source membership degrees are fused via a logical AND operation to semantically modulate token-level alignment, effectively suppressing interference from unobservable or noisy tokens and achieving fine-grained, robust cross-modal token-level alignment. By combining CDA and FTA, our framework simultaneously achieves adaptive sample-level alignment and robust fine-grained token-level alignment, effectively bridging the semantic gap between text and aerial images.

### 3.2. Context-Aware Dynamic Alignment

We propose a Context-Aware Dynamic Alignment (CDA) module to tackle the cross-modal alignment challenges caused by the visual discrepancies in aerial images. This module leverages ground-view images as auxiliary guidance, and quantify the alignment difficulty of text-ground and text-aerial, dynamically adjusts the weighting between direct alignment and ground-assisted bridged alignment. Specifically, given the global text features  $T^C \in \mathbb{R}^{B \times D}$ , global aerial image features  $A^C \in \mathbb{R}^{B \times D}$ , and global ground image features  $G^C \in \mathbb{R}^{B \times D}$ , we first compute the cross-modal similarity differences for each sample:

$$\Delta_i = \text{sim}(\mathbf{T}_i^C, \mathbf{A}_i^C) - \text{sim}(\mathbf{T}_i^C, \mathbf{G}_i^C), \quad i = 1, \dots, B, \quad (1)$$

where  $\text{sim}(\cdot, \cdot)$  denotes the cosine similarity. Intuitively,  $\Delta_i > 0$  indicates that direct alignment is likely sufficient, whereas  $\Delta_i < 0$  implies that a bridge via ground-level images is necessary. To enable dynamic alignment, we map the similarity discrepancy to a continuous coefficient  $\alpha_i \in [0, 1]$  using a nonlinear, context-sensitive activation:

$$\alpha_i = \frac{1}{1 + \exp[-k \cdot \Delta_i]}, \quad (2)$$

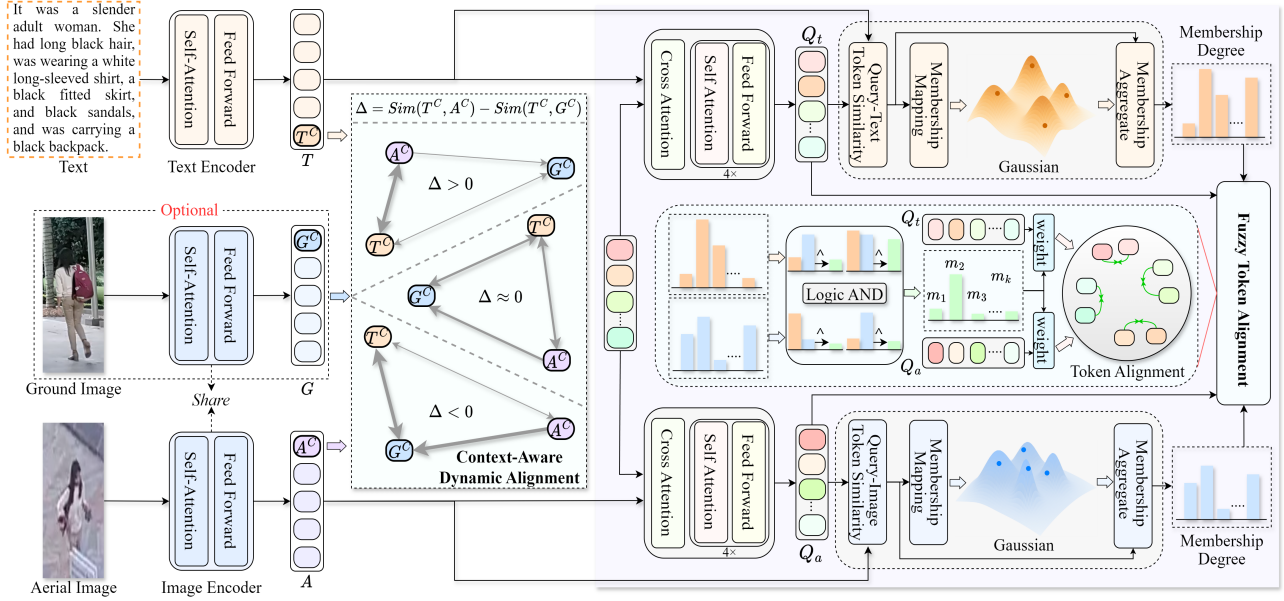


Figure 2. Overview of the proposed Cross-Modal Fuzzy Alignment Network.

where  $k$  is a sensitivity hyperparameter controlling the steepness of the mapping. Conceptually,  $\alpha_i$  functions as a soft decision gate, where samples with high direct similarity ( $\text{sim}(\mathbf{T}_i^C, \mathbf{A}_i^C) \gg \text{sim}(\mathbf{T}_i^C, \mathbf{G}_i^C)$ ) yield  $\alpha_i \rightarrow 1$ , emphasizing direct text-aerial alignment, whereas samples with low direct similarity ( $\text{sim}(\mathbf{T}_i^C, \mathbf{A}_i^C) \ll \text{sim}(\mathbf{T}_i^C, \mathbf{G}_i^C)$ ) yield  $\alpha_i \rightarrow 0$ , emphasizing bridge-based alignment via ground images. Therefore, the loss of this module is defined as:

$$\mathcal{L}_{\text{CAD}} = \frac{1}{B} \sum_{i=1}^B \left[ \alpha_i \cdot \mathcal{L}_{\text{direct}}(\mathbf{T}_i^C, \mathbf{A}_i^C) + (1 - \alpha_i) \cdot \mathcal{L}_{\text{bridge}}(\mathbf{T}_i^C, \mathbf{G}_i^C, \mathbf{A}_i^C) \right], \quad (3)$$

where  $\mathcal{L}_{\text{direct}}$  denotes the direct alignment loss between text and aerial image, and  $\mathcal{L}_{\text{bridge}}$  represents the indirect alignment of text and aerial features via a ground-level image as a semantic bridge. Both alignment terms are implemented using the SDM loss [13]:

$$\mathcal{L}_{\text{direct}}(\mathbf{T}_i^C, \mathbf{A}_i^C) = \text{SDM}(\mathbf{T}_i^C, \mathbf{A}_i^C), \quad (4)$$

$$\mathcal{L}_{\text{bridge}}(\mathbf{T}_i^C, \mathbf{G}_i^C, \mathbf{A}_i^C) = \text{SDM}(\mathbf{T}_i^C, \mathbf{G}_i^C) + \text{SDM}(\text{sg}(\mathbf{G}_i^C), \mathbf{A}_i^C), \quad (5)$$

where  $\text{sg}()$  means stop-gradient operator, which prevents backpropagation through the ground-level features, ensuring that the aerial features are adaptively aligned toward the ground bridge without altering the ground representation.

This design enables each sample to dynamically balance direct and bridge-mediated alignment, effectively mitigating cross-modal alignment challenges caused by variations in visual cues. Moreover, when ground images are unavailable, the CDA loss degenerates to the standard SDM loss.

### 3.3. Fuzzy Token Alignment

To address fine-grained misalignment between text and aerial person images, we propose the Fuzzy Token Alignment (FTA) module, grounded in fuzzy logic theory to quantify token reliability within each modality. Tokens with low membership are considered unreliable and their contribution to cross-modal alignment is suppressed, whereas tokens with high membership in both modalities are preserved, enabling precise alignment.

Given textual features  $\mathbf{T} \in \mathbb{R}^{B \times N_t \times D}$  and aerial image features  $\mathbf{A} \in \mathbb{R}^{B \times N_a \times D}$ , we introduce a shared learnable query  $\mathbf{Q} \in \mathbb{R}^{K \times D}$  to interact with both modalities and map them into a unified semantic space:

$$\mathbf{Q}_a = \text{CrossFormer}(\mathbf{Q}, \mathbf{A}, \mathbf{A}), \quad (6)$$

$$\mathbf{Q}_t = \text{CrossFormer}(\mathbf{Q}, \mathbf{T}, \mathbf{T}), \quad (7)$$

where  $\text{CrossFormer}$  denotes the cross-modal interaction module, composed of a cross-attention layer followed by multiple self-attention and feed-forward layers, producing modality-aware query representations  $\mathbf{Q}_t, \mathbf{Q}_a \in \mathbb{R}^{B \times K \times D}$ .

To measure the reliability of each query token, we use the global class token of the corresponding modality as a semantic reference, and quantify the token's reliability with

a learnable Gaussian scale parameter. Taking the image modality as an example, we first predict the Gaussian scale  $\sigma$  from the global class token  $\mathbf{A}^C \in \mathbb{R}^D$  using an MLP:

$$\log \sigma = \text{MLP}(\mathbf{A}^C), \quad \sigma = \exp(\log \sigma). \quad (8)$$

Next, for each query token, we compute its overall similarity to the class token  $r_j$ , and map it to a membership degree  $\mu_j^a$  using a Gaussian function. This membership degree reflects the reliability of the token in the image modality:

$$r_j = \frac{Q_a^{(j)} \cdot A^C}{|Q_a^{(j)}|_2 |A^C|_2}, \quad \mu_j^a = \exp\left(-\frac{(1-r_j)^2}{2\sigma^2}\right). \quad (9)$$

The membership  $\mu_j^t$  for the text modality is computed similarly. In this way, each token’s membership  $\mu_j \in [0, 1]$  not only reflects its alignment with the global semantic representation, but also quantifies the token’s reliability for cross-modal alignment, the higher the value, the more the token can be trusted; the lower the value, the more likely it is noisy or uninformative and should be suppressed.

We then fuse token-level memberships from both modalities using a fuzzy logic AND operation:

$$\mu_j^{\text{joint}} = \mu_j^a \cdot \mu_j^t, \quad (10)$$

where we adopt the multiplicative form as a differentiable soft AND operator, which emphasizes tokens with high confidence in both modalities while allowing gradient-based optimization. Only tokens with high reliability in both modalities retain strong influence during cross-modal alignment. The token-level cosine similarity is then weighted by the joint membership to obtain the sample-level similarity:

$$s_j = \frac{q_a^{(j)\top} q_t^{(j)}}{|q_a^{(j)}|_2 |q_t^{(j)}|_2}, \quad \text{sim}(Q_a, Q_t) = \frac{1}{K} \sum_{j=1}^K \mu_j^{\text{joint}} s_j. \quad (11)$$

The text-image similarity  $\text{sim}(Q_t, Q_a)$  is computed similarly. Using these bidirectional weighted similarities, we further employ the similarity distribution matching [13] to compute the fuzzy token alignment loss  $L_{\text{FTA}}$ .

$$p_{i,j} = \frac{\exp(\text{sim}(Q_a^i, Q_t^j)/\tau)}{\sum_{k=1}^N \exp(\text{sim}(Q_a^i, Q_t^k)/\tau)}, \quad q_{i,j} = \frac{y_{i,j}}{\sum_{k=1}^N y_{i,k}}, \quad (12)$$

$$\mathcal{L}_{\text{FTA}} = \frac{1}{2} \sum_{i=1}^N \sum_{j=1}^N \left[ p_{i,j} \log \frac{p_{i,j}}{q_{i,j} + \epsilon} + p_{j,i} \log \frac{p_{j,i}}{q_{j,i} + \epsilon} \right], \quad (13)$$

where  $\tau$  is a temperature hyperparameter,  $\epsilon$  is used to prevent numerical instability during computation. This mechanism ensures that only tokens that are reliably present in both modalities contribute significantly to alignment, suppressing noisy or weak tokens and enabling precise and robust fine-grained cross-modal alignment.

## 4. Benchmark

### 4.1. Overview

To advance research on text-aerial person retrieval, we construct a large-scale benchmark, AERI-PEDES. The person images in this dataset are collected from three distinct aerial-ground person re-identification datasets [28–30], where each identity naturally contains multiple images from both ground and aerial viewpoints. To reduce manual annotation costs while ensuring the accuracy of captions, we propose a Chain-of-Though (CoT) based caption generation framework to produce high-quality captions. In the test set, all captions are manually annotated to provide a reliable evaluation benchmark that closely reflects real-world scenarios. Figure 3(a) illustrates several examples from AERI-PEDES.

### 4.2. CoT-based Caption Generation Framework

Existing caption generation methods based on multimodal large language models often suffer from attribute omission and visual hallucination. To address these issues, we propose a CoT based generation framework, as illustrated in Figure 4, which improves both the granularity and verifiability of generated captions. Specifically, a perception model  $f_{\text{percep}}$  first performs structured visual parsing on the input image  $I$ , extracting visible attributes  $\mathbf{A} = a_1, \dots, a_n$  along with their supporting visual evidence  $\mathbf{V}$  and confidence scores ( $\mathbf{C}$ , forming an intermediate representation  $T_1 = (\mathbf{A}, \mathbf{V}, \mathbf{C})$ ). These attributes are then organized into an initial caption  $S_{\text{init}}$  with a recorded reasoning trace, yielding  $T_2 = (S_{\text{init}}, \text{trace}_{\text{gen}})$ . To correct potential omissions or errors, a secondary model  $f_{\text{corr}}$  performs vision-guided auditing on  $(I, S_{\text{init}})$ , producing a refined caption  $S_{\text{refined}}$  and a correction trace, resulting in the final state  $T_3 = (S_{\text{refined}}, \text{trace}_{\text{corr}})$ . This progressive CoT mechanism effectively integrates visual parsing and auditing to preserve fine-grained attribute details while ensuring that the generated captions remain consistent with visual evidence. Further implementation details are provided in the **supplementary material**.

### 4.3. Benchmark Properties and Statistics

We construct AERI-PEDES, a large-scale cross-view benchmark with 4,659 identities, generated using a CoT-based captioning framework. The training set includes 3,659 identities, 112,672 aerial images, 26,351 ground images, and 26,213 generated captions, while the test set contains 1,000 identities, 5,525 aerial images, and 6,141 manually annotated captions for reliable evaluation. As shown in Table 1, compared with other person retrieval datasets, AERI-PEDES offers larger scale, broader cross-platform coverage, and richer scene diversity. The captions are detailed, with a maximum length of 108 words and an av-

Table 1. Comparison AERI-PEDES with other datasets for text-image person retrieval.

Datasets		AERI-PEDES	TBAPR [38]	CUHK-PEDES [23]	ICFG-PEDES [7]	RSTPReid [48]
Image	Number	144,548	65,880	40,206	54,522	20,505
	Ground & Aerial	✓	✓	×	×	×
	Multi-Sources	✓	✓	✓	×	×
Caption	Average Length	38.6	56.1	23.5	37.2	25.8
	Maximum Length	105	87	96	83	70
	Generated (Train) & Human (Test)	✓	×	×	×	×

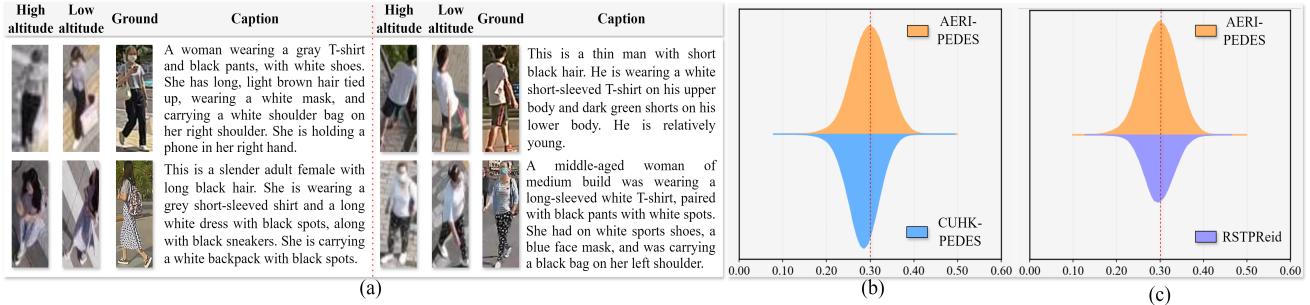


Figure 3. (a) Illustrates sample data from the AERI-PEDES benchmark. (b) Shows the text-image similarity distribution in comparison with CUHK-PEDES. (c) Shows the text-image similarity distribution in comparison with RSTPReid.

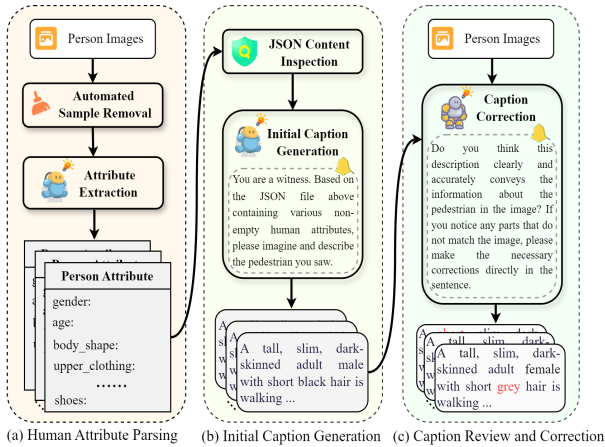


Figure 4. Chain-of-Thought Based Caption Generation Framework.

erage of 38.6 words; only the training captions are generated, whereas the test captions remain manually annotated to better reflect real-world usage. We further analyze the CLIP-based image-text similarity distributions (Figure 3(b)(c)). Unlike fully manual datasets such as CUHK-PEDES and RSTPReid, AERI-PEDES exhibits a wider similarity spread, demonstrating the effectiveness of the CoT captioning framework in producing high-quality, semantically consistent descriptions.

## 5. Experiments

### 5.1. Datasets and Evaluation Metrics

**Datasets.** We evaluate our method on the AERI-PEDES and TBAPR [38].

**TBAPR** is the first benchmark specifically designed for text-aerial person retrieval. It contains 65,880 person images, with the training set comprising 1,180 identities and the test set containing 529 identities.

**Evaluation Metrics.** We evaluate our method using multiple widely adopted retrieval metrics, including Rank-k ( $k=1, 5, 10$ ), mAP (Mean Average Precision) and RSum (Sum of Rank), detailed introductions are provided in the **supplementary material**.

### 5.2. Implementation Details

CFAN uses the CLIP text encoder for textual feature extraction, while aerial and ground images share a CLIP-based visual encoder initialized with the pre-trained weights provided by Jiang et al [14]. Image data are processed with standard augmentation operations and uniformly resized to  $384 \times 128$ , while text inputs are enhanced via random masking to improve model robustness. The cross-modal interaction query in the FTA module consists of 4 learnable 512-dimensional tokens. The model is trained using the Adam optimizer for 60 epochs with an initial learning rate of  $5 \times 10^{-6}$  and a cosine decay schedule. The batch size is set to 64, and training is conducted on a single RTX 4090

Table 2. Comparison results on the AERI-PEDES, and TBAPR datasets.

Method	Ref	AERI-PEDES					TBAPR				
		Rank-1	Rank-5	Rank-10	mAP	RSum	Rank-1	Rank-5	Rank-10	mAP	RSum
IRRA [13]	CVPR23	35.14	53.23	63.19	33.42	151.57	39.63	58.72	67.69	35.31	166.04
APTМ [44]	MM23	34.62	53.95	64.5	31.09	153.07	43.59	62.03	69.75	38.71	175.37
RDE [32]	CVPR24	38.56	58.26	67.89	37.16	164.71	37.31	54.06	60.75	32.17	152.12
CFAM [49]	CVPR24	30.77	51.37	61.61	30.4	143.75	48.34	66.31	73.21	42.67	184.78
NAM [36]	CVPR24	42.47	61.72	69.99	40.22	174.17	46.56	63.13	70.13	40.92	179.82
VFE [34]	KBS25	35.76	55.35	65.56	35.35	156.67	47.94	62.5	68.17	42.18	178.63
DM-Adpeter [25]	AAAI25	33.42	53.17	62.79	32.41	149.37	37.81	58.34	66.56	33.28	162.71
LPNC [37]	TIFS25	35.65	53.61	63.69	35.19	152.95	41.78	58.03	65.50	37.87	165.31
LPNC+Pretrain [37]	TIFS25	43.79	61.49	70.40	42.22	175.68	45.41	62.31	69.94	42.17	177.66
AEA-FIRM [38]	TCSVT25	37.94	56.66	65.71	34.89	160.31	44.75	62.38	69.13	36.28	176.26
AEA-FIRM+Pretrain [14]	TCSVT25	44.42	61.96	71.03	41.12	177.41	48.15	63.87	71.21	42.01	183.23
HAM [14]	CVPR25	44.58	63.52	72.67	42.45	180.77	47.81	64.96	72.53	41.86	185.30
Ours (W/O Ground)	-	45.06	64.53	73.21	43.27	182.80	49.15	65.88	73.47	42.89	188.50
Ours (With Ground)	-	47.16	65.66	73.83	44.79	186.65	49.47	66.50	73.06	43.96	189.03

GPU.

### 5.3. Comparison with State-of-the-Art Methods

**Performance Comparison on the AERI-PEDES Datasets.** As shown in Table 2, we conduct a comprehensive evaluation of the proposed method on the AERI-PEDES dataset and perform detailed comparisons with existing state-of-the-art approaches. Specifically, AEA-FIRM, as the first attempt targeting text–aerial person alignment, demonstrates certain advantages over traditional text–image person retrieval methods on AERI-PEDES. However, due to the extremely large viewpoint variations in this benchmark, the difficulty of cross-modal alignment is significantly amplified. Even with strong pretrained models, AEA-FIRM only achieves 44.42% Rank-1 accuracy, 41.12% mAP, and 177.41% RSum, performing on par with HAM. In contrast, our method delivers substantial performance improvements. Under the non-ground-assisted setting, it already surpasses all competing approaches. When ground-view images are further incorporated as auxiliary cues, our method sets a new state of the art, achieving 47.16% Rank-1, 44.79% mAP, and 186.65% RSum, representing nearly a 6% gain in RSum over the previous best method. These results highlight the superior capability of our approach in handling cross-modal alignment under extreme viewpoint disparities. While existing methods struggle in this challenging scenario, our model benefits from fuzzy logic based token-level reliability modeling, enabling more accurate and robust fine-grained cross-modal alignment.

**Performance Comparison on the TBAPR Datasets.** On the TBAPR dataset, our method consistently outperforms all compared approaches across all evaluation metrics. Specifically, without using ground-view images, our

Table 3. Ablation experiments of different components on AERI-PEDES dataset.

Methods	Rank-1	Rank-5	Rank-10	mAP	RSum
Baseline	43.88	61.11	69.85	41.58	174.84
+ CDA	46.18	64.40	72.46	43.98	183.04
+ FTA	44.55	61.77	70.32	41.89	176.64
+ CDA + FTA	47.16	65.66	73.83	44.79	186.65

method already achieves 49.15% Rank-1 accuracy and 42.89% mAP, surpassing all competing methods. When ground-view images are further incorporated as auxiliary information, our method reaches a new SoTA, achieving 66.50% Rank-5 and 189.03% RSum. It is worth noting that, since the TBAPR dataset contains many low-altitude aerial images, the visual differences between aerial and ground-view images are relatively small. This allows direct alignment between text and aerial images to achieve strong performance, limiting the auxiliary contribution of ground images. In contrast, our method can further improve results thanks to the CDA module, which adaptively balances the contributions of text–aerial and text–ground alignment. This enables robust cross-modal semantic matching and effectively leveraging ground-view information.

### 5.4. Ablation Study

In this section, we evaluate each component of CFAN using the baseline model with ground-image assisted bridge alignment loss for comparison.

**Effectiveness of the Context-Aware Dynamic Alignment Loss.** As shown in Table 3, using only bridge alignment (baseline) achieves 43.88% Rank-1, 41.58% mAP, and 174.84% RSum. However, although bridge align-

Table 4. Impact of Different Bridge Modalities in CDA.

Bridge	Rank-1	Rank-5	Rank-10	mAP	RSum
None	45.06	64.53	73.21	43.27	182.80
Aerial	46.08	64.60	73.33	44.20	184.01
Ground	47.16	65.66	73.83	44.79	186.65

ment alleviates the semantic gap between aerial images and text, it fails to fully exploit direct alignment for low-difficulty samples, leading to suboptimal matching performance. After introducing the CDA loss, key metrics improve significantly, with RSum increasing by 8.2%, along with corresponding gains in Rank-1 and mAP. This improvement is mainly attributed to CDA, which dynamically estimates alignment difficulty and adaptively balances direct and bridge alignment. Specifically, low-difficulty samples emphasize direct alignment, while high-difficulty samples rely more on bridge alignment, thereby enhancing overall alignment accuracy and robustness.

**Effectiveness of the Fuzzy Token Alignment.** As shown in Table 3, incorporating the FTA module into the baseline yields improvements of 0.67%, 0.31%, and 1.2% in Rank-1, mAP, and RSum, respectively. Further integrating FTA on top of the CDA loss leads to additional gains of 0.98%, 0.81%, and 3.61%. These improvements mainly stem from the Fuzzy Token Alignment module, which modulates fine-grained token correspondences through fuzzy membership and suppresses interference from unobservable or noisy tokens during token-level alignment. Consequently, only reliable and semantically supported tokens participate in cross-modal matching, resulting in more accurate alignment.

**Impact of Different Bridge in CDA.** As shown in Table 4, “None” indicates no intermediate bridge, “Aerial” uses low-altitude aerial images of the same identity, and “Ground” uses ground-level images. Introducing a bridge (Aerial or Ground) consistently improves performance, showing that intermediate modalities help ease cross-modal alignment. Aerial images provide noticeable gains, while Ground images achieve the best results due to higher semantic consistency with text. The small gap between Aerial and Ground suggests that CDA does not strictly rely on ground images and can flexibly use different bridge modalities for robust alignment.

### 5.5. Parameter Sensitivity Analysis

We conduct an ablation study on the number of tokens in the learnable query  $Q$ . As shown in Figure 5, we evaluated the effect of varying the token count from 1 to 16. The results indicate that changes in token number have little impact on the mAP metric. When the number of token is set to 4, the model achieves the highest RSum performance of 186.65%. However, further increasing the number of tokens leads to performance degradation, likely due to redundancy and in-

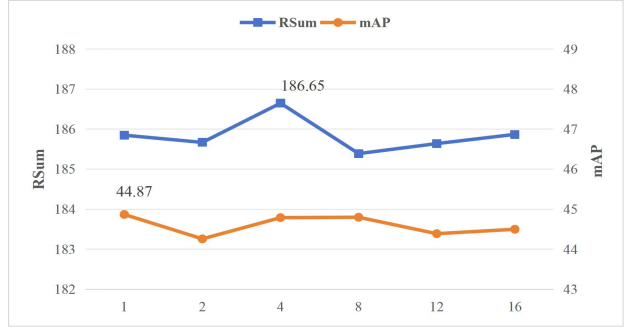


Figure 5. Impact of the Number of Learnable Query Tokens.

Table 5. Sensitivity analysis of the hyperparameter  $k$  in the context-aware dynamic alignment module.

$k$	1	2	4	8	12	16
Rank-1	47.16	46.91	47.04	46.77	46.23	46.04
mAP	44.79	44.58	44.50	43.83	43.70	43.55
RSum	186.65	185.88	185.91	184.11	183.99	183.31

terference among tokens caused by over-parameterization, which weakens fine-grained cross-modal alignment. Based on these observations, we set the number of learnable query tokens to 4 in our final configuration.

We further analyze the sensitivity of the hyperparameter  $k$  in the CDA module. As shown in Table 5, the best performance is achieved at  $k$ , while larger  $k$  values lead to a gradual decline. This is because increasing  $k$  makes the Sigmoid function overly steep, resulting in overly extreme weighting between direct and bridge alignment, which weakens fine-grained adjustment and degrades overall performance.

## 6. Conclusion

In this paper, we propose a Cross-modal Fuzzy Alignment Network for text-aerial person retrieval, aimed at addressing the challenges of cross-modal alignment arising from degraded visual cues in aerial images. Firstly, we introduce a Fuzzy Token Alignment module, which leverages fuzzy logic to quantify token-level reliability, enabling accurate and robust fine-grained alignment between text and aerial image features. Secondly, we design a Context-Aware Dynamic Alignment module, which incorporates ground-view images as a bridging mechanism to effectively reduce alignment discrepancies between text and aerial images, adaptively balancing direct and bridge-assisted alignment for each sample. In addition, we construct AERI-PEDES, a large-scale benchmark dataset generated with a chain-of-thought approach. Multi-stage prompts produce attribute parsing, initial captions, and refined descriptions with traceable intermediate states, ensuring high accuracy, completeness, and visual consistency of the generated captions. Extensive experiments demonstrate the superior effectiveness and robustness of our method.

## References

- [1] Mohsen Ahmadi, Fatemeh Dashti Ahangar, Nikoo Astaraki, Mohammad Abbasi, and Behzad Babaei. Fwnnet: Presentation of a new classifier of brain tumor diagnosis based on fuzzy logic and the wavelet-based neural network using machine-learning methods. *Computational Intelligence and Neuroscience*, 2021(1):8542637, 2021.
- [2] Fei-Long Chen, Du-Zhen Zhang, Ming-Lun Han, Xiu-Yi Chen, Jing Shi, Shuang Xu, and Bo Xu. Vlp: A survey on vision-language pre-training. *Machine Intelligence Research*, 20:38–56, 2023.
- [3] Yuhao Chen, Guoqing Zhang, Yujiang Lu, Zhenxing Wang, and Yuhui Zheng. Tipcb: A simple but effective part-based convolutional baseline for text-based person search. *Neurocomputing*, 494:171–181, 2022.
- [4] Yifei Deng, Zhengyu Chen, Chenglong Li, and Jin Tang. Uncertainty-aware coarse-to-fine alignment for text-image person retrieval. *Visual Intelligence*, 3(1):6, 2025.
- [5] Yifei Deng, Chenglong Li, Futian Wang, and Jin Tang. Learning hierarchical cross-modal association with intra-modal context for text-image person retrieval. In *Proceedings of the 33rd ACM International Conference on Multimedia*, pages 2723–2731, 2025.
- [6] Weiping Ding, Mohamed Abdel-Basset, Hossam Hawash, and Witold Pedrycz. Multimodal infant brain segmentation by fuzzy-informed deep learning. *IEEE Transactions on Fuzzy Systems*, 30(4):1088–1101, 2021.
- [7] Zefeng Ding, Changxing Ding, Zhiyin Shao, and Dacheng Tao. Semantically self-aligned network for text-to-image part-aware person re-identification. *arXiv preprint arXiv:2107.12666*, 2021.
- [8] Zhaodong Ding, Chenglong Li, Tao Wang, and Futian Wang. Quality-aware spatio-temporal transformer network for rgbt tracking. *IEEE Transactions on Image Processing*, 34:7845–7858, 2025.
- [9] Siyuan Duan, Yuan Sun, Dezhong Peng, Zheng Liu, Xiaomin Song, and Peng Hu. Fuzzy multimodal learning for trusted cross-modal retrieval. In *Proceedings of the Computer Vision and Pattern Recognition Conference*, pages 20747–20756, 2025.
- [10] Chanho Eom and Bumsub Ham. Learning disentangled representation for robust person re-identification. *Advances in neural information processing systems*, 32, 2019.
- [11] Adem Golcuk. Hybrid fuzzy expert system and difference equation software filter for biomedical sensors. *IEEE Transactions on Instrumentation and Measurement*, 71:1–12, 2022.
- [12] Cosimo Ieracitano, Nadia Mammone, Mario Versaci, Giuseppe Varone, Abder-Rahman Ali, Antonio Armentano, Grazia Calabrese, Anna Ferrarelli, Lorena Turano, Carmela Tebala, et al. A fuzzy-enhanced deep learning approach for early detection of covid-19 pneumonia from portable chest x-ray images. *Neurocomputing*, 481:202–215, 2022.
- [13] Ding Jiang and Mang Ye. Cross-modal implicit relation reasoning and aligning for text-to-image person retrieval. In *Proceedings of the IEEE/CVF Conference on Computer Vision and Pattern Recognition*, pages 2787–2797, 2023.
- [14] Jiayu Jiang, Changxing Ding, Wentao Tan, Junhong Wang, Jin Tao, and Xiangmin Xu. Modeling thousands of human annotators for generalizable text-to-image person re-identification. In *Proceedings of the Computer Vision and Pattern Recognition Conference*, pages 9220–9230, 2025.
- [15] Jiandong Jin, Xiao Wang, Yin Lin, Chenglong Li, Lili Huang, Aihua Zheng, and Jin Tang. Sequencepar: Understanding pedestrian attributes via a sequence generation paradigm. *Pattern Recognition*, page 112356, 2025.
- [16] Jiandong Jin, Xiao Wang, Qian Zhu, Haiyang Wang, and Chenglong Li. Pedestrian attribute recognition: A new benchmark dataset and a large language model augmented framework. In *Proceedings of the AAAI Conference on Artificial Intelligence*, pages 4138–4146, 2025.
- [17] Ya Jing, Chenyang Si, Junbo Wang, Wei Wang, Liang Wang, and Tieniu Tan. Pose-guided multi-granularity attention network for text-based person search. In *Proceedings of the AAAI Conference on Artificial Intelligence*, pages 11189–11196, 2020.
- [18] Boyi Li, Yifan Shen, Yuanzhe Liu, Yifan Xu, Jiateng Liu, Xinzhuo Li, Zhengyuan Li, Jingyuan Zhu, Yunhan Zhong, Fangzhou Lan, et al. Toward cognitive supersensing in multimodal large language model. *arXiv preprint arXiv:2602.01541*, 2026.
- [19] Junnan Li, Ramprasaath Selvaraju, Akhilesh Gotmare, Shafiq Joty, Caiming Xiong, and Steven Chu Hong Hoi. Align before fuse: Vision and language representation learning with momentum distillation. *Advances in neural information processing systems*, 34:9694–9705, 2021.
- [20] Junnan Li, Dongxu Li, Silvio Savarese, and Steven Hoi. Blip-2: Bootstrapping language-image pre-training with frozen image encoders and large language models. In *International conference on machine learning*, pages 19730–19742. PMLR, 2023.
- [21] Kunchi Li, Hongyang Chen, Jun Wan, and Shan Yu. Ckdf-v2: Effectively alleviating representation shift for continual learning with small memory. *IEEE Transactions on Neural Networks and Learning Systems*, 2025.
- [22] Kunchi Li, Chaoyue Ding, Jun Wan, and Shan Yu. Enhance the old representations’ adaptability dynamically for exemplar-free continual learning. *Neurocomputing*, page 130286, 2025.
- [23] Shuang Li, Tong Xiao, Hongsheng Li, Bolei Zhou, Dayu Yue, and Xiaogang Wang. Person search with natural language description. In *Proceedings of the IEEE conference on computer vision and pattern recognition*, pages 1970–1979, 2017.
- [24] Lei Liu, Chenglong Li, Yun Xiao, Rui Ruan, and Minghao Fan. Rgbt tracking via challenge-based appearance disentanglement and interaction. *IEEE Transactions on Image Processing*, 33:1753–1767, 2024.
- [25] Yating Liu, Zimo Liu, Xiangyuan Lan, Wenming Yang, Yaowei Li, and Qingmin Liao. Dm-adapter: Domain-aware mixture-of-adapters for text-based person retrieval. In *Proceedings of the AAAI Conference on Artificial Intelligence*, pages 5703–5711, 2025.
- [26] Haoyu Lu, Yuqi Huo, Mingyu Ding, Nanyi Fei, and Zhiwu Lu. Cross-modal contrastive learning for generalizable and

- efficient image-text retrieval. *Machine Intelligence Research*, 20:569–582, 2023.
- [27] Yang Nan, Javier Del Ser, Zeyu Tang, Peng Tang, Xiaodan Xing, Yingying Fang, Francisco Herrera, Witold Pedrycz, Simon Walsh, and Guang Yang. Fuzzy attention neural network to tackle discontinuity in airway segmentation. *IEEE transactions on neural networks and learning systems*, 35(6):7391–7404, 2023.
- [28] Huy Nguyen, Kien Nguyen, Sridha Sridharan, and Clinton Fookes. Ag-reid. v2: Bridging aerial and ground views for person re-identification. *IEEE Transactions on Information Forensics and Security*, 19:2896–2908, 2024.
- [29] Huy Nguyen, Kien Nguyen, Akila Pemasiri, Feng Liu, Sridha Sridharan, and Clinton Fookes. Ag-vpreid: A challenging large-scale benchmark for aerial-ground video-based person re-identification. In *Proceedings of the Computer Vision and Pattern Recognition Conference*, pages 1241–1251, 2025.
- [30] Kien Nguyen, Clinton Fookes, Sridha Sridharan, Feng Liu, Xiaoming Liu, Arun Ross, Dana Michalski, Huy Nguyen, Debayan Deb, Mahak Kothari, et al. Ag-reid 2023: Aerial-ground person re-identification challenge results. In *2023 IEEE International Joint Conference on Biometrics (IJB)*, pages 1–10. IEEE, 2023.
- [31] Song-Liang Pan, Kunchi Li, Da-Han Wang, Xu-Yao Zhang, Jiantao Liu, and Shunzhi Zhu. Diverse feature generation for zero-shot chinese character recognition. *Expert Systems with Applications*, page 129442, 2025.
- [32] Yang Qin, Yingke Chen, Dezhong Peng, Xi Peng, Joey Tianyi Zhou, and Peng Hu. Noisy-correspondence learning for text-to-image person re-identification. In *Proceedings of the IEEE/CVF Conference on Computer Vision and Pattern Recognition*, pages 27197–27206, 2024.
- [33] Alec Radford, Jong Wook Kim, Chris Hallacy, Aditya Ramesh, Gabriel Goh, Sandhini Agarwal, Girish Sastry, Amanda Askell, Pamela Mishkin, Jack Clark, et al. Learning transferable visual models from natural language supervision. In *International conference on machine learning*, pages 8748–8763. Pmlr, 2021.
- [34] Wei Shen, Ming Fang, Yuxia Wang, Jiafeng Xiao, Diping Li, Huangqun Chen, Ling Xu, and Weifeng Zhang. Enhancing visual representation for text-based person searching. *Knowledge-Based Systems*, 309:112893, 2025.
- [35] Yifan Shen, Yuanzhe Liu, Jingyuan Zhu, Xu Cao, Xiaofeng Zhang, Yixiao He, Wenming Ye, James Matthew Rehg, and Ismini Lourentzou. Fine-grained preference optimization improves spatial reasoning in vlms. *arXiv preprint arXiv:2506.21656*, 2025.
- [36] Wentan Tan, Changxing Ding, Jiayu Jiang, Fei Wang, Yibing Zhan, and Dapeng Tao. Harnessing the power of mllms for transferable text-to-image person reid. In *Proceedings of the IEEE/CVF Conference on Computer Vision and Pattern Recognition*, pages 17127–17137, 2024.
- [37] Xueping Wang, Hao Wu, Min Liu, and Yaonan Wang. Learnable prompts with neighbor-aware correction for text-based person search. *IEEE Transactions on Information Forensics and Security*, 2025.
- [38] Yihao Wang, Meng Yang, Rui Cao, and Guangwei Gao. Aea-firm: Adaptive elastic alignment with fine-grained representation mining for text-based aerial pedestrian retrieval. *IEEE Transactions on Circuits and Systems for Video Technology*, 2025.
- [39] Zhe Wang, Zhiyuan Fang, Jun Wang, and Yezhou Yang. Vitaa: Visual-textual attributes alignment in person search by natural language. In *Computer vision—ECCV 2020: 16th European conference, glasgow, UK, August 23–28, 2020, proceedings, part XII 16*, pages 402–420. Springer, 2020.
- [40] Jason Wei, Xuezhi Wang, Dale Schuurmans, Maarten Bosma, Fei Xia, Ed Chi, Quoc V Le, Denny Zhou, et al. Chain-of-thought prompting elicits reasoning in large language models. *Advances in neural information processing systems*, 35:24824–24837, 2022.
- [41] Feng Xu, Guangyao Zhai, Xin Kong, Tingzhong Fu, Daniel FN Gordon, Xueli An, and Benjamin Busam. Stare-vla: Progressive stage-aware reinforcement for fine-tuning vision-language-action models. *arXiv preprint arXiv:2512.05107*, 2025.
- [42] Yang Xu, Yifan Feng, Xu Zhuang, Jason Wang, Zongze Wu, and Yue Gao. Residual fuzzy alignment on hypergraph for open-set 3d cross-modal retrieval. *IEEE Transactions on Multimedia*, 2025.
- [43] Shuanglin Yan, Neng Dong, Liyan Zhang, and Jinhui Tang. Clip-driven fine-grained text-image person re-identification. *IEEE Transactions on Image Processing*, 32:6032–6046, 2023.
- [44] Shuyu Yang, Yinan Zhou, Zhedong Zheng, Yaxiong Wang, Li Zhu, and Yujiao Wu. Towards unified text-based person retrieval: A large-scale multi-attribute and language search benchmark. In *Proceedings of the 31st ACM International Conference on Multimedia*, pages 4492–4501, 2023.
- [45] Lotfi A Zadeh. Fuzzy sets. *Information and control*, 8(3):338–353, 1965.
- [46] Xiaowei Zhao, Chenglong Li, Jin Tang, and Chuanfu Li. Learning with Explicit Topological Priors for Chest X-ray Rib Segmentation. In *proceedings of Medical Image Computing and Computer Assisted Intervention – MICCAI 2025*. Springer Nature Switzerland, 2025.
- [47] Zhedong Zheng, Liang Zheng, Michael Garrett, Yi Yang, Mingliang Xu, and Yi-Dong Shen. Dual-path convolutional image-text embeddings with instance loss. *ACM Transactions on Multimedia Computing, Communications, and Applications (TOMM)*, 16(2):1–23, 2020.
- [48] Aichun Zhu, Zijie Wang, Yifeng Li, Xili Wan, Jing Jin, Tian Wang, Fangqiang Hu, and Gang Hua. Dssl: Deep surroundings-person separation learning for text-based person retrieval. In *Proceedings of the 29th ACM international conference on multimedia*, pages 209–217, 2021.
- [49] Jialong Zuo, Hanyu Zhou, Ying Nie, Feng Zhang, Tianyu Guo, Nong Sang, Yunhe Wang, and Changxin Gao. Ufinebench: Towards text-based person retrieval with ultra-fine granularity. In *Proceedings of the IEEE/CVF Conference on Computer Vision and Pattern Recognition*, pages 22010–22019, 2024.